Thermochimica Acta 497 (2010) 27–34

Contents lists available at ScienceDirect

Thermochimica Acta

journal homepage: www.elsevier.com/locate/tca

# Curing kinetics and mechanisms of polysulfone nanofibrous membranes toughened epoxy/amine systems using isothermal DSC and NIR

Gang Li[a], Zhibin Huang[b], Peng Li[b], Chunling Xin[a], Xiaolong Jia[b], Binghui Wang[b], Yadong He[a,*], Seungkon Ryu[c], Xiaoping Yang[b]

[a] College of Mechanical and Electrical Engineering, Beijing University of Chemical Technology, Beijing 100029, PR China
[b] The Key Laboratory of Beijing City on Preparation and Processing of Novel Polymer Materials, Beijing University of Chemical Technology, Beijing 100029, PR China
[c] Department of Chemical Engineering, Chungnan National University, Daejeon 305-764, South Korea

ARTICLE INFO

*Article history:*
Received 28 April 2009
Received in revised form 9 August 2009
Accepted 11 August 2009
Available online 19 August 2009

*Keywords:*
Curing kinetics
Polysulfone nanofibrous membrane
Epoxy
Differential scanning calorimetry (DSC)
Near infra-red (NIR)

ABSTRACT

Curing kinetics and mechanisms of polysulfone nanofibrous membranes toughened TGDDM/DDS were investigated by using isothermal DSC and NIR, and compared to those of TGDDM/DDS and PSF films toughened TGDDM/DDS. At early curing stage, the curing rate of nanofibrous membranes toughened system was faster than those of other two systems, whereas the final conversion of toughened systems was lower than that of resin matrix. Most of the primary amine was consumed by gelation and the concentration of secondary amine reached the maximum around gelation. The faster consuming rates of primary and secondary amines in nanofibrous membranes toughened system resulted in higher concentration of hydroxyl groups and tertiary amines at gelation, which led to larger amounts of branching and crosslinking compared to resin matrix. The comparison of the results obtained from two methods showed that the epoxide conversion exhibited identical variations as a function of time, as well as the curing rate.



## 1. Introduction

The tetrafunctional epoxy resin tetraglycidyl-4,4′-diaminodiphenylmethane (TGDDM), cured with 4,4′-diaminodiphenyl sulfone (DDS), was one of the most widely employed matrices for high performance fibre composites in aerospace applications [1,2]. To improve the inherent brittleness resulted from the highly crosslinking density, thermoplastics have been usually used to toughen the epoxy/amine systems [3,4]. However, the incorporation of thermoplastics in toughened systems would produce further complexities due to reaction-induced phase separation during the curing process, which may affect the curing rates and structural transformations, such as gelation and vitrification in epoxy/amine reactions [5–7].

In our previous work, the inhomogeneous phase separation of polysulfone (PSF) resulted from the special structure of electrospun nanofibrous membranes has been generated [8]. Large porosity and high specific surface area of nanofibrous membranes have allowed them easily impregnated by epoxy matrix to increase the compatibility [9,10]. Thus the curing rate of nanofibrous membranes toughened epoxy/amine systems might be increased due to the enhanced mobility of the crosslinking network and higher content of amine hardener in epoxy rich phase [11,12], which were attributed to the mutual plasticization between the continuous epoxy phase and the dispersed PSF phase. Besides resin/hardener themselves, the crosslinking network structure was also influenced by the curing kinetic parameters according to the reaction mechanism [13,14]. Therefore, it is necessary to understand the curing kinetics and mechanisms of PSF nanofibrous membranes toughened epoxy/amine systems, which were associated directly with final network structure and in turn ultimate properties of cured composite.

A number of methods have been used to study the curing process of epoxy/amine systems. Differential scanning calorimetry (DSC) was a useful technique because it allowed the direct measurement of the heat flow [11,15,16], which was directly proportional to the curing rate as well as the epoxide conversion in isothermal DSC. However, only the curing kinetics of overall reaction could be obtained by DSC. Fortunately, near infra-red (NIR) spectroscopy has been successfully used in the quantitative analysis of the curing reaction of epoxy/amine systems [13,17,18]. The major functional groups involved in the curing process, such as epoxy, primary and secondary amine, and hydroxyl functional groups, could be isolated well from the neighboring absorptions in the NIR spectrum. By monitoring the conversions of these functional groups during the curing process, the reaction mechanisms and the resul-

* Corresponding author. Tel.: +86 10 64452920; fax: +86 10 64452920.
*E-mail address:* heyd@mail.buct.edu.cn (Y. He).

0040-6031/$ – see front matter © 2009 Elsevier B.V. All rights reserved.
doi:10.1016/j.tca.2009.08.005

tant structural features could be analyzed as well as the curing kinetics.

Therefore, in this study, the isothermal curing process of PSF nanofibrous membranes toughened TGDDM/DDS were investigated by DSC and NIR, respectively, and compared to those of TGDDM/DDS and PSF films toughened TGDDM/DDS. The DSC data were modeled by autocatalytic mechanism and advanced isoconversional method. The NIR data were used to study the curing kinetics of different functional groups involved in the epoxy/amine curing process, and further to analyze the reaction mechanisms. Also, the results obtained from these two methods were compared.

## 2. Experimental

### 2.1. Materials

The epoxy resin used in this study was tetrafunctional tetraglycidyl 4,4′-diaminodiphenylmethane (TGDDM, AG-80, Shanghai Institute of Synthetic Resins). The hardener used was 4,4′-diaminodiphenyl sulfone (DDS, YinSheng Chemical Limited Co., China). Polysulfone (PSF, Udel P1700, Amoco Co.) was used as a toughener. N,N′-dimethylacetamide (DMAC), acetone and dichloromethane were used as solvents.

### 2.2. Sample preparation

The resin matrix was prepared by dissolving 30 g of DDS in 100 g of TGDDM at 130 °C with vigorous mechanical stirring. After complete dissolution, the mixture was degassed under vacuum at the same temperature. PSF nanofibrous membranes and films were prepared according to our previous work [8]: PSF solution was prepared by dissolving 25 g PSF pellets in 90 ml DMAC and 10 ml acetone, and electrospun to obtain PSF nanofibrous membranes. PSF solution in dichloromethane was poured onto a glass plate and cast by Gardener knife to obtain PSF films. PSF nanofibrous membranes and films were covered on resin matrix, and the amount of PSF nanofibrous membranes and films was controlled to 5.0 wt%, respectively.

**Table 1**
DSC data of resin matrix, 5 wt% PSF nanofibrous membranes and films toughened epoxy.

| Sample | $T$ (°C) | $\Delta H_T$ (J/g) | $\Delta H_R$ (J/g) | $\Delta H_{total}$ (J/g) | $\alpha$ (%) |
|---|---|---|---|---|---|
| Resin matrix | 180 | 416.7 | 105.8 | 522.5 | 79.8 |
| | 190 | 485.2 | 91.5 | 576.7 | 84.2 |
| | 200 | 530.5 | 68.6 | 599.1 | 88.5 |
| PSF nanofibrous membranes toughened epoxy | 180 | 401.3 | 157.6 | 558.9 | 71.8 |
| | 190 | 419.7 | 157.6 | 560.4 | 74.9 |
| | 200 | 475.1 | 69.0 | 544.1 | 87.3 |
| PSF films toughened epoxy | 180 | 405.5 | 150.4 | 555.9 | 72.9 |
| | 190 | 438.7 | 101.4 | 540.1 | 81.2 |
| | 200 | 455.9 | 56.6 | 512.5 | 88.2 |

### 2.3. Differential scanning calorimetry

Resin matrix, 5.0 wt% PSF nanofibrous membranes and films toughened epoxy (5–8 mg) were sealed in aluminium pans, respectively. The reaction heats ($\Delta H_T$) of the samples were measured by differential scanning calorimetry (DSC, PerkinElmer, PYRIS 1) at 180, 190, and 200 °C in nitrogen atmosphere. Pure indium was used as a standard for calorimetric calibration. After the isothermal curing measurements, the samples were scanned again at 10 K/min to obtain the residual heats ($\Delta H_R$).

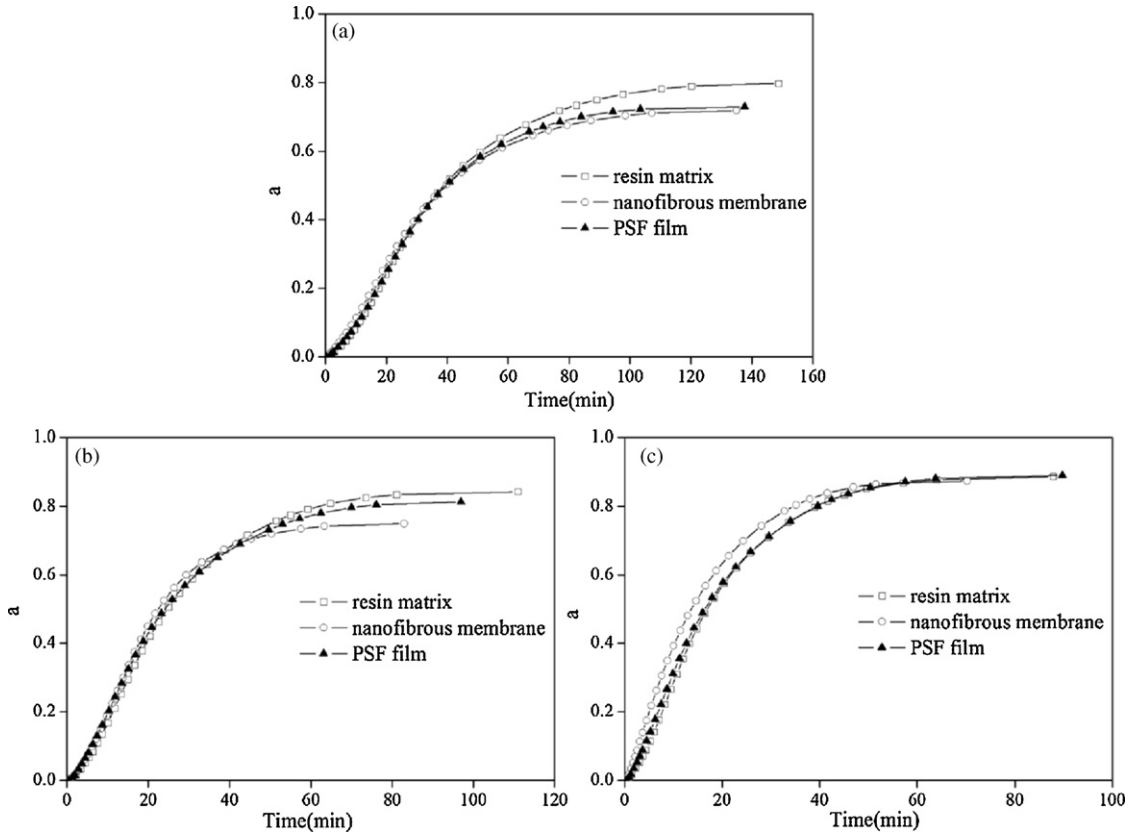


**Fig. 1.** The epoxide conversion of resin matrix, 5 wt% PSF nanofibrous membranes and films toughened epoxy cured at (a) 180 °C, (b) 190 °C, and (c) 200 °C as a function of time.

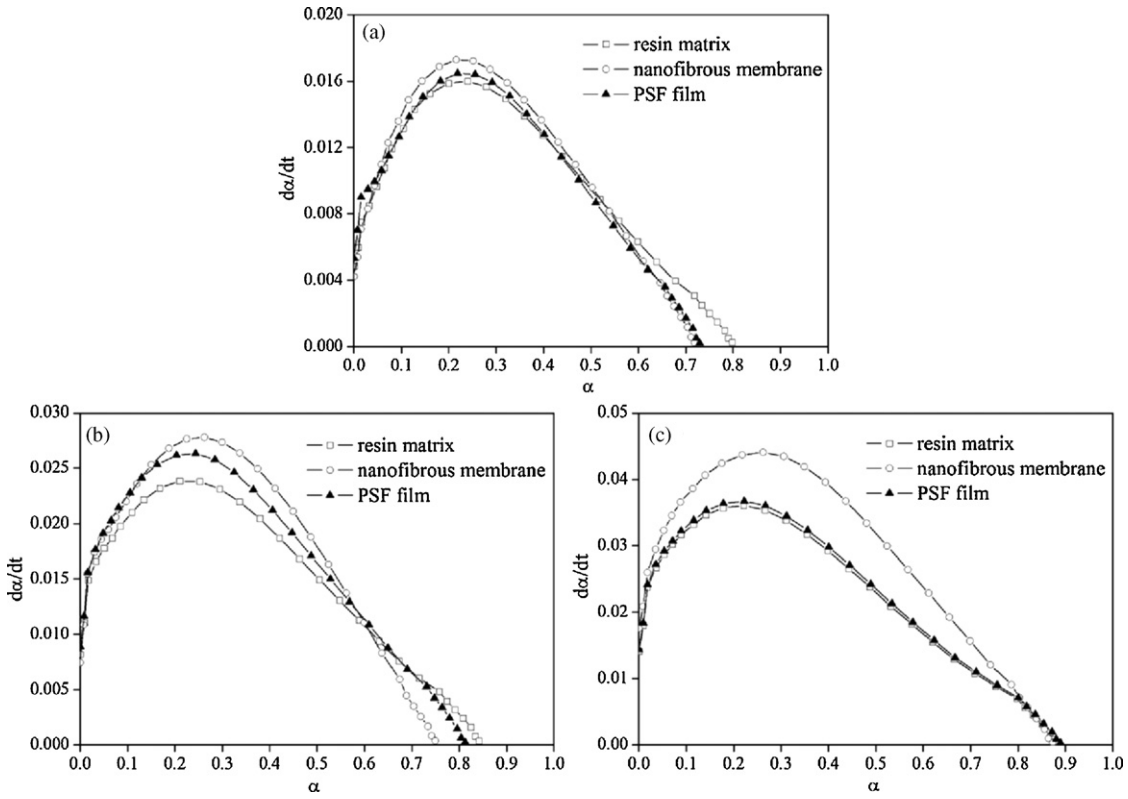


**Fig. 2.** The curing rate of resin matrix, 5 wt% PSF nanofibrous membranes and films toughened epoxy cured at (a) 180 °C, (b) 190 °C, and (c) 200 °C as a function of epoxide conversion.

### 2.4. Near infra-red spectroscopy

Resin matrix, 5.0 wt% PSF nanofibrous membranes and films toughened epoxy were inserted between two layers of KBr slices. The samples were isothermally cured at 190 °C, and removed at appropriate time intervals to monitor ranges of curing time. The transmission near infra-red spectroscopy (NIR) of the samples was performed using FT-IR spectrophotometer (Nicolet Instruments, Nexus 670, USA), which recorded spectra in the region from 7000 to 4000 $cm^{-1}$. The degree of thermal curing was determined from DSC testing, according to the method by Varley et al. [17].

## 3. Results and discussion

### 3.1. Isothermal DSC analysis

Table 1 shows the isothermal DSC data of resin matrix, 5 wt% PSF nanofibrous membranes and films toughened epoxy. $\Delta H_T$ is the reaction heat at constant temperature, $\Delta H_R$ is the residual heat of the reaction, and $\Delta H_{total}$ is the total heat of the reaction. The epoxide conversion ($\alpha$) and the curing rate ($d\alpha/dt$) were calculated from the following equations [11,19]:

$$\alpha = \frac{\Delta H_T}{\Delta H_{total}} \quad (1)$$

$$\frac{d\alpha}{dt} = \frac{1}{\Delta H_{total}} \times \frac{dH}{dt} \quad (2)$$

Fig. 1 shows the epoxide conversion of resin matrix, 5 wt% PSF nanofibrous membranes and films toughened epoxy cured at 180, 190, and 200 °C as a function of time. The conversion exhibited a rapid increase at the early stage of curing, subsequently a gradual increase above $\alpha = 0.6$ conversion, and finally remained constant due to the vitrification at the late stage of curing. Sbirrazzuoli et al. [16] have reported similar results. However, their $\alpha$ value was 0.4, which was lower than our data due to the different resin system and curing conditions. The conversion became faster as the temperature higher, and the constant value increased nearly 0.9 as the increase of temperature. The conversion rates of toughened systems were a little faster at early curing stage at 180 and 190 °C than that of resin matrix, while that of PSF nanofibrous membrane was far faster than those of others at 200 °C. At the end of curing, the final epoxide conversions of PSF nanofibrous membranes and films toughened epoxy were lower than that of resin matrix at 180 and 190 °C, which were attributed to the partitioning of epoxy resin in epoxy rich phase and PSF rich phase [19]. In toughened systems, the miscibility between epoxy and PSF led to the reduction of the overall amount of epoxy resin in epoxy rich phase. Therefore, the far less reactivity of epoxy resin in PSF rich phase resulted in the decrease of the epoxide conversion.

Fig. 2 shows the curing rate of resin matrix, 5 wt% PSF nanofibrous membranes and films toughened epoxy cured at 180, 190, and 200 °C as a function of epoxide conversion. At constant temperature, the curing rate increased with the increase of epoxide conversion, and reached maximum at around $\alpha = 0.25$ conversion, then decreased gradually to zero. At the same conversion, the curing rate increased with increasing the temperature. The rate curves were distinctly autocatalytic in nature [14,20,21]. Obviously, the addition of PSF did not change the autocatalytic characteristic of the curing reaction. However, the curing rates of PSF nanofibrous membranes and films toughened epoxy were clearly enhanced at lower conversion, which were due to the enhanced mobility of the network resulted from the plasticization of the continuous epoxy phase by PSF [11]. With the increase of the conversion, the curing rate of toughened system was lower than that of resin matrix.

According to the above discussion, the curing reaction of three systems followed the autocatalytic mechanism. The autocatalytic kinetic expression was proposed by Horie as following equation

**Table 2**
Isothermal curing kinetics parameters of resin matrix, 5 wt% PSF nanofibrous membranes and films toughened epoxy.

| $T$ (°C) | $k_1 \times 10^3$ (min$^{-1}$) | $k_2 \times 10^3$ (min$^{-1}$) | $m$ | $n$ | $m+n$ |
|---|---|---|---|---|---|
| Resin matrix | | | | | |
| 180 | 4.86 | 46.22 | 0.40 | 1.57 | 1.97 |
| 190 | 8.19 | 65.99 | 0.57 | 1.46 | 2.03 |
| 200 | 14.11 | 92.75 | 0.53 | 1.43 | 1.96 |
| PSF nanofibrous membranes toughened epoxy | | | | | |
| 180 | 7.37 | 65.21 | 0.6 | 1.45 | 2.05 |
| 190 | 11.48 | 91.68 | 0.57 | 1.51 | 2.08 |
| 200 | 17.54 | 126.97 | 0.53 | 1.46 | 1.99 |
| PSF films toughened epoxy | | | | | |
| 180 | 5.33 | 55.31 | 0.47 | 1.55 | 2.02 |
| 190 | 8.91 | 78.35 | 0.47 | 1.68 | 2.15 |
| 200 | 14.38 | 109.29 | 0.43 | 1.41 | 1.84 |

[14,21]:

$$\frac{d\alpha}{dt} = (k_1 + k_2\alpha^m)(1-\alpha)^n \quad (3)$$

where $d\alpha/dt$ is the curing rate, $\alpha$ is the epoxide conversion, $m$ and $n$ are variables to determine the reaction order, $k_1$ and $k_2$ are the apparent rate coefficients for the reaction catalyzed by proton donors initially present in the system and produced during the curing process, respectively.

The constant $k_1$ can be calculated from the initial curing rate at $\alpha = 0$ in Fig. 2. To obtain the reaction order $n$, Eq. (3) can be described as follows:

$$\ln\left(\frac{d\alpha}{dt}\right) = \ln(k_1 + k_2\alpha^m) + n\ln(1-\alpha) \quad (4)$$

Therefore, the first estimate of $n$ can be obtained from the slope of the plot of $\ln(d\alpha/dt)$ versus $\ln(1-\alpha)$. Then Eq. (3) can be further rearranged as follows:

$$\ln\left[\frac{d\alpha/dt}{(1-\alpha)^n} - k_1\right] = \ln k_2 + m\ln\alpha \quad (5)$$

The first term of Eq. (5) can be computed by the previously estimated $k_1$, and $n$ values. The left-hand terms of Eq. (5) versus $\ln\alpha$ was plotted with linearity, then the reaction order $m$ and the constant $k_2$ can be estimated by the slope and intercept of the straight line. By applying the above procedures, preliminary kinetic parameters can be obtained on the first trial. However, an iterative procedure should be used to obtain more precise values. Eq. (3) can also be rearranged as follows:

$$\ln\left[\frac{d\alpha/dt}{k_1 + k_2\alpha^m}\right] = n\ln(1-\alpha) \quad (6)$$

With $k_2$, $m$, and $n$ estimated from the above procedures, the left-hand terms of Eq. (6) can be plotted versus $\ln(1-\alpha)$, and a new value of the reaction order $n$ can be obtained from the slope. This new value of $n$ is compared with the one obtained earlier and the same iterative procedure can be repeated until the convergence of $m$ and $n$ values within 1% deviation was achieved.

Table 2 shows the isothermal curing kinetics parameters of resin matrix, 5 wt% PSF nanofibrous membranes and films toughened epoxy obtained from the above procedures. The reaction orders, $m$ and $n$, were approximately 0.4–0.6 and 1.4–1.7, respectively. And the orders did not vary a lot for three systems. With increase in the temperature, the apparent rate coefficients $k_1$ and $k_2$ increased, indicating the increase of the curing rate. The results indicated that the early curing rate of nanofibrous membranes toughened epoxy was the fastest, which was agreed well with the above results. The $k_1$ mainly governed the early stage of autocatalytic reaction, and $k_2$ affected the reaction after the initial stage. Therefore, the curing rate increase might be more pronounced as the reaction proceeded beyond the initial stage, which was very similar to the variation tendency of curing rate in thermoplastics toughened epoxy systems [11].

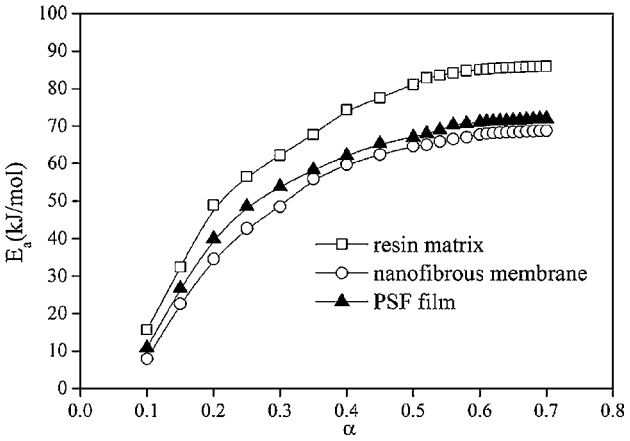


**Fig. 3.** The activation energy of resin matrix, 5 wt% PSF nanofibrous membranes and films toughened epoxy as a function of epoxide conversion.

However, the autocatalytic mechanism could not describe the end of the curing reaction which was known to be diffusion-controlled due to gelation and vitrification [22]. Fortunately, the advanced isoconversional method developed by Vyazovkin [23,24] was very effective in detecting the complexity of the curing reaction, and further evaluating the activation energy as a function of the epoxide conversion ($\alpha$). According to this method, for a set of $n$ experiments carried out at different arbitrary heating programs, $T_i(t)$, the activation energy was determined at any particular value of $\alpha$ by finding the value of $E_\alpha$ that minimized the function [23,24].

$$\Phi(E_\alpha) = \sum_{i=1}^{n}\sum_{j\neq i}^{n}\frac{J[E_\alpha, T_i(t_\alpha)]}{J[E_\alpha, T_j(t_\alpha)]} \quad (7)$$

In the above equation, the integral [23,24]:

$$J[E_\alpha, T_i(t_\alpha)] = \int_0^{t_\alpha} \exp\left[\frac{-E_\alpha}{RT_i(t)}\right] dt \quad (8)$$

was determined by with the help of a Doyle's approximation [25]:

$$J[E_\alpha, T_i(t_\alpha)] \cong \frac{E}{R}\exp\left(-5.331 - 1.052\frac{E}{RT_i(t)}\right) \quad (9)$$

Fig. 3 shows the activation energy ($E_\alpha$) of resin matrix, 5 wt% PSF nanofibrous membranes and films toughened epoxy as a function of epoxide conversion ($\alpha$). The value of activation energy ranged from 10 to 80 kJ/mol, which was typical for epoxy–amine reaction. At early stage of curing, the smaller energy barrier of the segment motion resulted in the fast curing rate. However, more energy was required to overcome the motion among molecule chains at later curing stages, which was attributed to the less mobility of the segment resulted from the diffusion-controlled reaction. In addition, the activation energy of toughened epoxy was slightly lower than that of resin matrix, indicating the increase of the curing rate in well agreement with the above results.

### 3.2. Isothermal NIR analysis

The NIR spectra of TGDDM and DDS are shown in Fig. 4. The strong peak at 4522 cm$^{-1}$ and weaker peaks at 5878 and 6068 cm$^{-1}$ were seen in TGDDM epoxy. The peak at 4522 cm$^{-1}$ was due to a combination of the epoxy CH fundamental at 3050 cm$^{-1}$ and the $CH_2$ fundamental at 1460 cm$^{-1}$ [17,26]. The peaks at 5878 and 6068 cm$^{-1}$ were due to the first overtones of the fundamental $CH_2$ and CH stretches, respectively. In DDS spectrum a primary

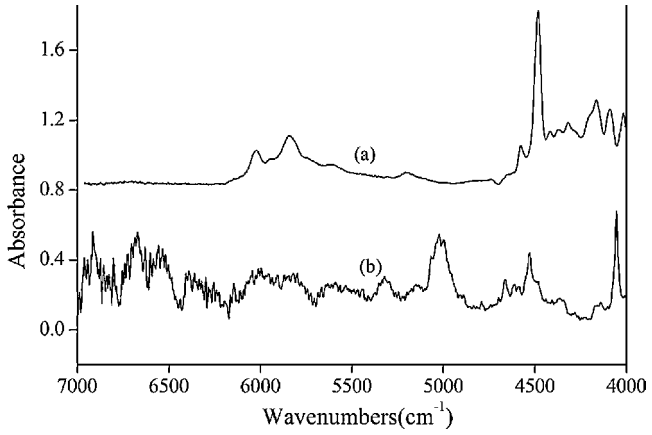


**Fig. 4.** NIR spectra of (a) TGDDM and (b) DDS.

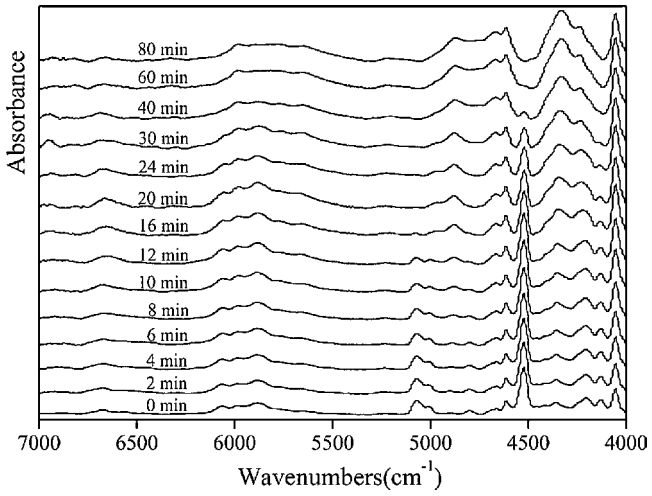


**Fig. 5.** NIR spectra of resin matrix cured at 190 °C as a function of time.

amine NH combination peak at 5072 $cm^{-1}$ and NH overtone peak at 6627 $cm^{-1}$ were observed. In the overtone regions an aromatic CH peak at 5991 $cm^{-1}$ was also found.

Figs. 5–7 show the NIR spectra of resin matrix, 5 wt% PSF nanofibrous membranes and films toughened epoxy cured at 190 °C as a function of time, respectively.

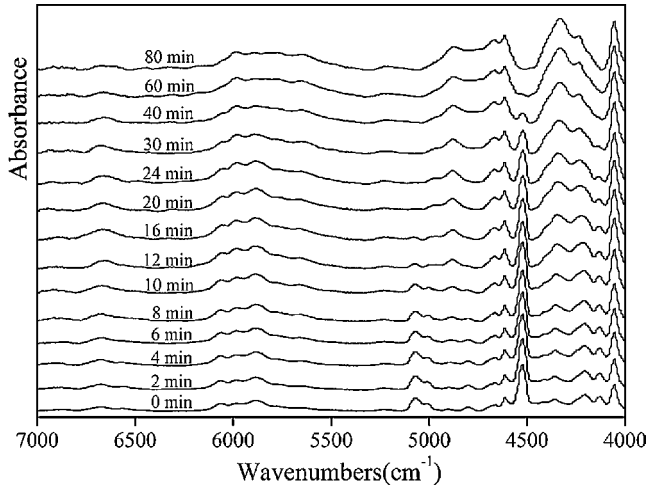


**Fig. 6.** NIR spectra of 5 wt% PSF nanofibrous membranes toughened epoxy cured at 190 °C as a function of time.

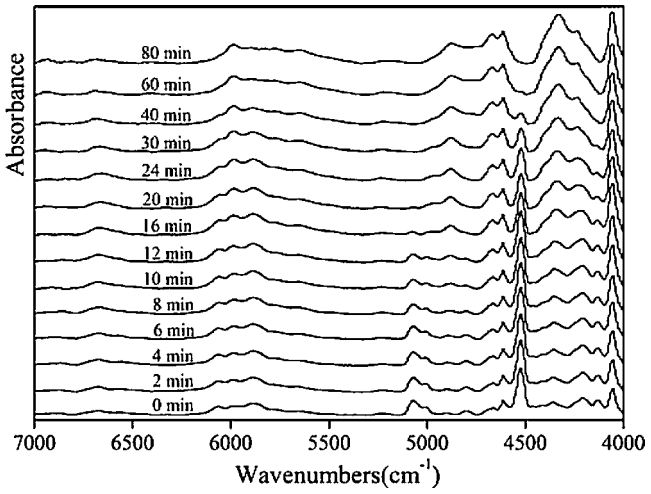


**Fig. 7.** NIR spectra of 5 wt% PSF films toughened epoxy cured at 190 °C as a function of time.

Scheme 1 shows three functional reactions that may be related to the spectral changes in above figures [16,27,28]. The first reaction, primary amine addition to epoxide, resulted in the decrease of the peak intensity at 4522 and at 5072 $cm^{-1}$, and final disappearance at the end of curing. The secondary amine generated from the first reaction may subsequently react with another epoxide group, to produce tertiary amine. This resulted in the growth, and reduction of bands in the region of 6577–6692 $cm^{-1}$, which were a combination of a primary and secondary amine overtone. The third possible reaction shown in Scheme 1, etherification, was competitive with the amine reactions but was more important at higher temperatures due to higher activation energy [16]. As a result, the hydroxyl peak at 4903 $cm^{-1}$ has grown at the expense of epoxy C–H peaks [13,29]. From the analysis of NIR spectra, the instantaneous information of the reactions during the network formation could be obtained. As reported previously [13,17], the aromatic CH overtone peak at 5991 $cm^{-1}$, which was not consumed or produced during the curing process, was chosen as an internal standard between different samples. Therefore, the conversion of epoxide groups and primary amine were calculated using the following equations [17,27,30]:

$$\alpha_{epoxy} = 1 - \frac{A_{4522,t}/A_{4522,0}}{A_{5991,t}/A_{5991,0}} \quad (10)$$

$$\alpha_{NH_2} = 1 - \frac{A_{5072,t}/A_{5072,0}}{A_{5991,t}/A_{5991,0}} \quad (11)$$

Primary amine-epoxy addition

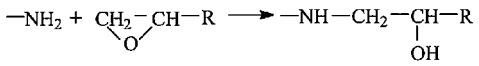

Secondary amine-epoxy addition

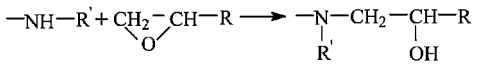

Hydroxyl-epoxy addition (etherification)

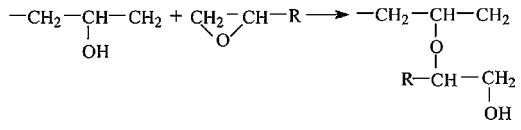

**Scheme 1.** Reactions occurred during the curing of TGDDM/DDS.

where $A_{4522}$ is the peak areas of the epoxide groups, $A_{5072}$ is the peak areas of the primary amine, $A_{5991}$ is the peak areas of the internal bands, and the subscripts $t$ and 0 are referenced to any curing time, $t = t$, and the initial time, $t = 0$, respectively.

As described by Min and Stachurski [13], the weight concentration of the component (expressed in mol/kg) can be calculated from the initial composition of the mixture. During the early stage of curing, the etherification could be neglected. So the concentration of secondary amine ($[SA]_t$) can be estimated according to the below equation [30,31]:

$$[SA]_t = 2([PA]_0 - [PA]_t) - ([EP]_0 - [EP]_t) \quad (12)$$

where $[PA]_0$ and $[EP]_0$ are the calculated concentration of primary amine and epoxide, $[PA]_t$ and $[EP]_t$ correspond to the concentrations of primary amine and epoxide after a certain curing time, $t$. And the concentration of tertiary amine can be obtained by the following equation [30,31]:

$$[TA]_t = [PA]_0 - [PA]_t - [SA]_t \quad (13)$$

The hydroxyl concentration can be readily calculated by assuming that the reaction between epoxide groups and primary or secondary amine was the only source of hydroxyl groups. The equation to calculate the hydroxyl concentration at time $t$, $[OH]_t$, is as follows [27,32]:

$$[OH]_t = [PA]_0 - [PA]_t + [TA]_t \quad (14)$$

Fig. 8 shows the epoxide conversions of resin matrix, 5 wt% PSF nanofibrous membranes and films toughened epoxy cured at 190 °C as a function of time. The increases of epoxide conversion of nanofibrous membranes and films toughened epoxy were faster than that of resin matrix, which indicated that the curing rates of nanofibrous membranes and films toughened epoxy were higher than that of resin matrix. The results were well consistent with those obtained from DSC in Fig. 1(b).

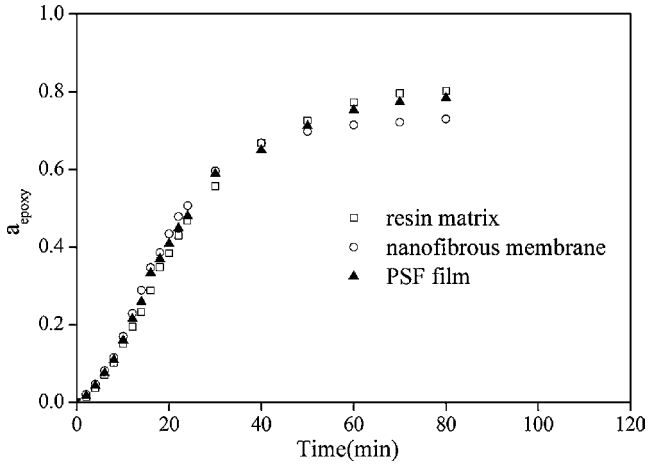


**Fig. 8.** The epoxide conversions of resin matrix, 5 wt% PSF nanofibrous membranes and films toughened epoxy cured at 190 °C as a function of time.

Fig. 9 shows the concentrations of three amine groups in resin matrix, 5 wt% PSF nanofibrous membranes and films toughened epoxy cured at 190 °C as a function of time. At the beginning of curing, the reaction mechanism was dominated by primary amine addition to epoxide, and the concentration of primary amine showed a rapid consumption. According to the Flory's equation [33], the gel point for TGDDM/DDS system corresponded to an epoxide conversion of 0.33. As shown in Fig. 8, the gel time for the conversion of 0.33 was about at 17–19 min. At this time most of the primary amine had been depleted by gelation, which

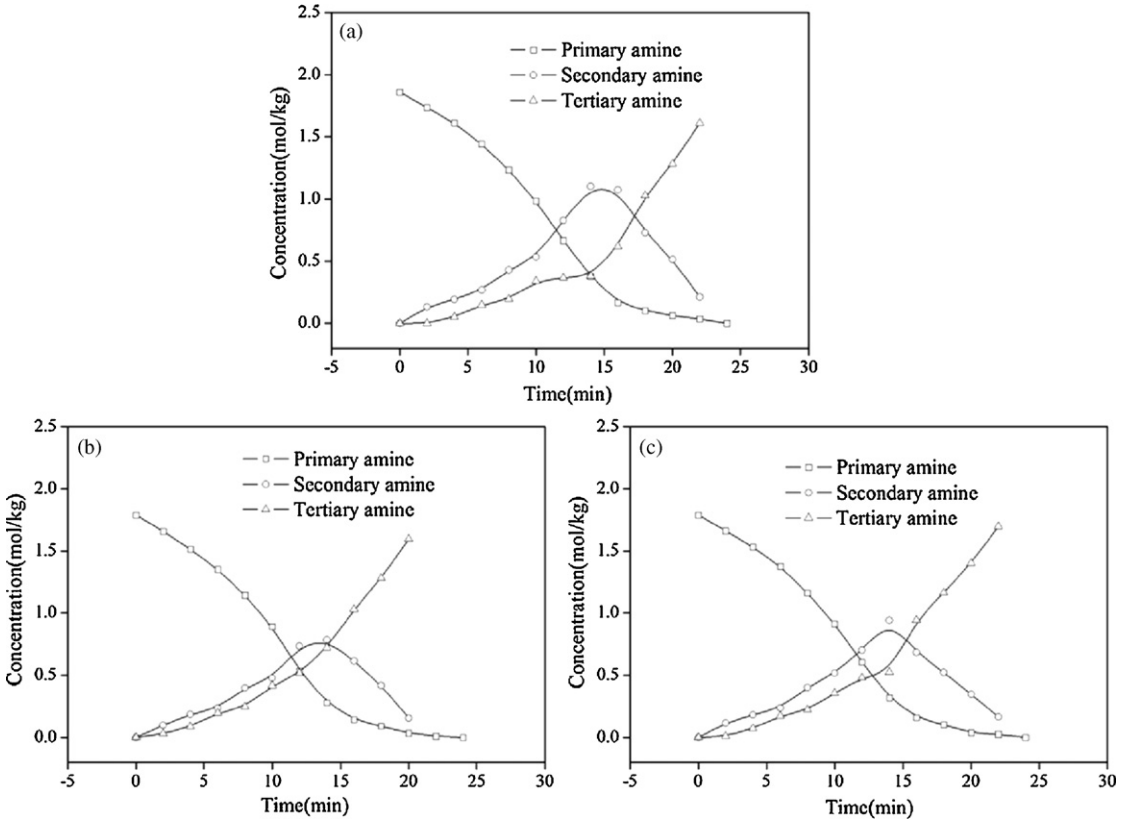


**Fig. 9.** Concentrations of three amine groups in (a) resin matrix, 5 wt% PSF (b) nanofibrous membranes and (c) films toughened epoxy cured at 190 °C as a function of time.

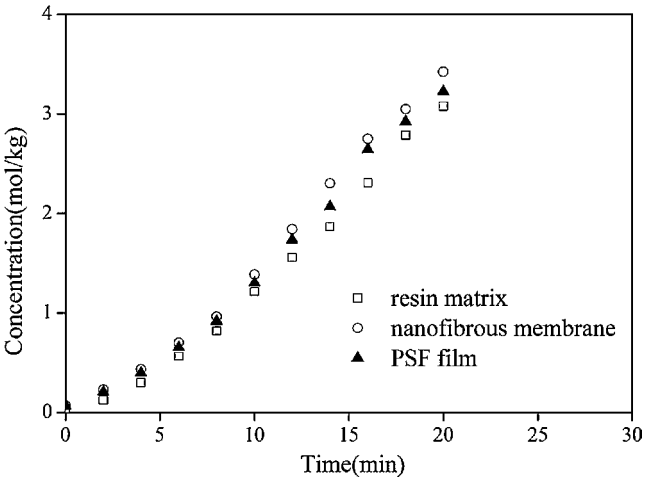


**Fig. 10.** Concentrations of hydroxyl groups in resin matrix, 5 wt% PSF nanofibrous membranes and films toughened epoxy cured at 190 °C as a function of time.

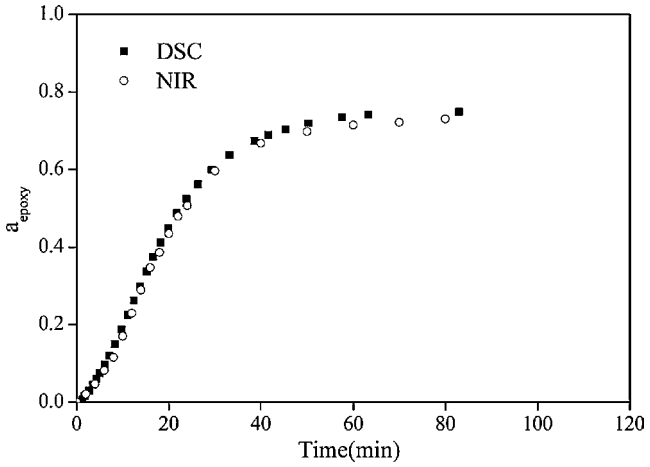


**Fig. 11.** Comparison of the epoxide conversion obtained from DSC with that of NIR for 5 wt% PSF nanofibrous membranes toughened epoxy cured at 190 °C as a function of time.

coincided with the results by St John and George [27]. The concentration of secondary amine reached the maximum near the gel point, and subsequently declined due to further reaction with other epoxide groups [28]. The concentration of tertiary amine at this point began to increase rapidly, thus resulting in the formation of three dimensional crosslinking network that in turn provided the significant increase in mechanical and thermal properties [34].

Fig. 10 shows the concentrations of hydroxyl groups in resin matrix, 5 wt% PSF nanofibrous membranes and films toughened epoxy cured at 190 °C as a function of time. As the primary and secondary amines were consumed, the hydroxyl functional groups were produced. The consuming rates of the primary and secondary amines of nanofibrous membranes and films toughened epoxy were faster than those of resin matrix, which resulted in the higher concentrations of hydroxyl groups and tertiary amines at gelation. Therefore, compared to resin matrix, much greater amounts of branching and crosslinking in toughened system occurred prior to gelation [17,27], which finally led to a lower level of epoxide conversion.

### 3.3. Comparison of isothermal DSC and NIR

Fig. 11 shows the comparison of the epoxide conversion obtained from DSC with that of NIR for 5 wt% PSF nanofibrous membranes toughened epoxy cured at 190 °C as a function of time. The conversions determined independently using DSC and NIR were almost identical. The conversion measured from NIR was consistently a little lower than that from DSC, which may be attributed to the repeated removement of the samples during NIR testing. However, the similarity of the conversion values indicated the validity of NIR analysis method, which was also proved by many researchers [6,17].

Fig. 12 shows the comparison of the curing rates obtained from DSC and NIR for resin matrix, 5 wt% PSF nanofibrous membranes and films toughened epoxy cured at 190 °C as a function of time. Obviously, the plots followed autocatalytic mechanism, and the variable tendency of the curing rates versus time from these two methods was identical. The curing rate of nanofibrous membranes toughened epoxy was the fastest, which was attributed to the best compatibility between nanofibrous membranes and epoxy. The plasticization of the continuous epoxy phase by nanofibrous membranes resulted in the enhancement of the mobility of the network [11,19]. Also, the plasticization of the dispersed PSF phase by epoxy led to an excess of amine groups in the epoxy rich phase, which resulted in the increase of the curing rate. However, as the curing proceeded, the curing rates of PSF nanofibrous membranes and films toughened epoxy were slower gradually than that of resin matrix, which was due to the phase separation in toughened systems. This in turn would increase the degree of other side reactions, such as etherification and homopolymerization, which resulted in a looser network with lower crosslinking density.

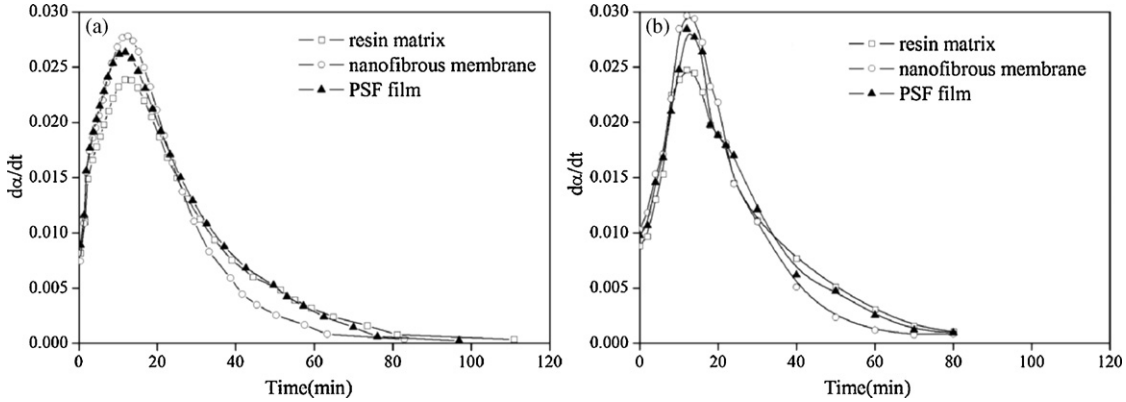


**Fig. 12.** Comparison of the curing rates obtained from (a) DSC and (b) NIR for resin matrix, 5 wt% PSF nanofibrous membranes and films toughened epoxy cured at 190 °C as a function of time.

## 4. Conclusions

The isothermal curing kinetics parameters of TGDDM/DDS, 5 wt% PSF nanofibrous membranes and films toughened TGDDM/DDS can be obtained both from DSC and NIR, and the epoxide conversion as well as the curing rate can be quantitively calculated and compared as a function of time by using theoretical equations. At the initial curing stage, the curing reaction of three systems followed the autocatalytic mechanism, and the activation energy dependence on different epoxide conversion can be calculated according to advanced isoconversional method. The primary amine addition to epoxide was the dominating reaction before gelation, resulting in the maximum concentration of secondary amine around gelation. The curing rates of PSF nanofibrous membranes and films toughened epoxy were faster than that of resin matrix, which was attributed to more consumption of the primary and secondary amine in toughened systems. The higher concentration of hydroxyl groups and tertiary amines at gelation resulted in much greater amounts of branching and crosslinking in PSF nanofibrous membranes toughened system, which finally led to lower epoxide conversion compared to PSF films toughened system and resin matrix.

## Acknowledgment

We would like to acknowledge the National Natural Science Foundation of China and the Natural Science Foundation of Beijing City (2093041) for supporting this project (50873010).

## References

[1] P. Musto, L. Mascia, G. Ragosta, G. Scarinzi, P. Villano, Polymer 41 (2000) 565–574.
[2] P. Musto, E. Martuscelli, G. Ragosta, P. Russo, P. Villano, J. Appl. Polym. Sci. 74 (1999) 532–540.
[3] I. Martinez, M.D. Martin, A. Eceiza, P. Oyanguren, I. Mondragon, Polymer 41 (2000) 1027–1035.
[4] B. Fernandez, A. Arbelaiz, E. Diaa, I. Mondragon, Polym. Compos. 25 (2004) 480–488.
[5] L. Bonnaud, J.P. Pascault, H. Sautereau, Eur. Polym. J. 36 (2000) 1313–1321.
[6] R.J. Varley, J.H. Hodgkin, G.P. Simon, Polymer 42 (2001) 3847–3858.
[7] P.A. Oyanguren, B. Aizpurua, M.J. Galante, J. Polym. Sci. B: Polym. Phys. 37 (1999) 2711–2725.
[8] G. Li, P. Li, C. Zhang, Y. Yu, H. Liu, S. Zhang, X. Jia, X. Yang, Z. Xue, S.K. Ryu, Compos. Sci. Technol. 68 (2008) 987–994.
[9] D. Li, Y. Xia, Adv. Mater. 16 (2004) 1151–1170.
[10] S. Ioannis, Chronakis, J. Mater. Process. Technol. 167 (2005) 283–293.
[11] C.C. Su, E.M. Woo, Polymer 36 (1995) 2883–2894.
[12] C.C. Su, J.F. Kuo, E.M. Woo, J. Polym. Sci. B: Polym. Phys. 33 (1995) 2235–2244.
[13] B.G. Min, Z.H. Stachurski, Polymer 34 (1993) 3620–3627.
[14] W.G. Kim, J.Y. Lee, Polymer 43 (2003) 5713–5722.
[15] S. Vyazovkin, N. Sbirrazzuoli, Macromolecules 29 (1996) 1867–1873.
[16] N. Sbirrazzuoli, A. Mititelu-Mija, L. Vincent, C. Alzina, Thermochim. Acta 447 (2006) 167–177.
[17] R.J. Varley, G.R. Heath, D.G. Hawthorne, J.H. Hodgkin, Polymer 36 (1995) 1347–1355.
[18] N. Poisson, G. Lachenal, H. Sautereau, Vib. Spectrosc. 12 (1996) 237–247.
[19] R.J. Varley, J.H. Hodgkin, D.G. Hawthorne, G.P. Simon, D. McCulloch, Polymer 41 (2001) 3425–3436.
[20] J.Y. Lee, M.J. Shimb, S.W. Kim, Thermochim. Acta 371 (2001) 45–51.
[21] S. Steven, G.V. Assche, W. Vuchelen, Macromolecules 38 (2005) 2281–2288.
[22] S. Vyazovkin, N. Sbirrazzuoli, Macromol. Chem. Phys. 200 (1999) 2294–2303.
[23] N. Sbirrazzuoli, S. Vyazovkin, Thermochim. Acta 388 (2002) 289–298.
[24] N. Sbirrazzuoli, S. Vyazovkin, A. Mititelu, C. Sladic, L. Vincent, Macromol. Chem. Phys. 204 (2003) 1815–1821.
[25] H. Cai, P. Li, G. Sui, Y. Yu, G. Li, X. Yang, S.K. Ryu, Thermochim. Acta 473 (2008) 101–105.
[26] Q. Wang, B.K. Storm, L.P. Houmler, J. Appl. Polym. Sci. 87 (2003) 2295–2305.
[27] N.A. St John, G.A. George, Polymer 33 (1992) 2679–2687.
[28] G. George, N. Hynard, G. Cash, L. Rintoul, M. O'Shea, C. R. Chimie 9 (2006) 1433–1443.
[29] G. Lachenal, I. Stevenson, A. Durand, G. Seytre, D. Bertrand, Macromol. Symp. 265 (2008) 249–259.
[30] A. Rigail-Cedeno, C.S.P. Sung, Polymer 46 (2005) 9378–9384.
[31] L. Xu, J.H. Fu, J.R. Schlup, Ind. Eng. Chem. Res. 35 (1996) 963–972.
[32] H. Liu, A. Uhlherr, R.J. Varley, M.K. Bannister, J. Polym. Sci. A: Polym. Chem. 42 (2004) 3143–3156.
[33] E.A. Mertze1, D.R. Perchak, W.M. Ritchey, J.L. Koenig, Ind. Eng. Chem. Res. 27 (1988) 580–586.
[34] R.J. Varley, W. Liu, G.P. Simon, J. Appl. Polym. Sci. 99 (2006) 3288–3299.